

Accepted Manuscript

Design and Synthesis of A Biaryl Series As Inhibitors for the Bromodomains of CBP/P300

Kwong Wah Lai, F. Anthony Romero, Vickie Tsui, Maureen H. Beresini, Gladys de Leon Boenig, Sarah M. Bronner, Kevin Chen, Zhongguo Chen, Edna F. Choo, Terry D. Crawford, Patrick Cyr, Susan Kaufman, Yingjie Li, Jiangpeng Liao, Wenfeng Liu, Justin Ly, Jeremy Murray, Weichao Shen, John Wai, Fei Wang, Caicai Zhu, Xiaoyu Zhu, Steven Magnuson

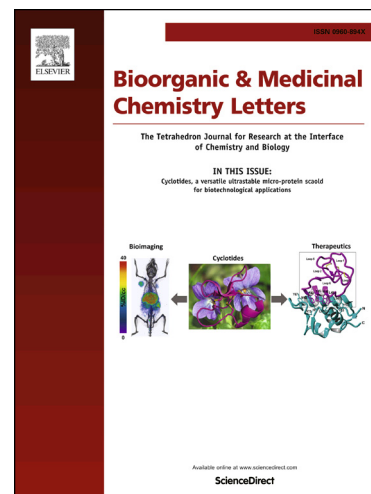
PII: S0960-894X(17)31113-7
DOI: <https://doi.org/10.1016/j.bmcl.2017.11.025>
Reference: BMCL 25431

To appear in: *Bioorganic & Medicinal Chemistry Letters*

Received Date: 1 September 2017
Revised Date: 7 November 2017
Accepted Date: 13 November 2017

Please cite this article as: Lai, K.W., Romero, F.A., Tsui, V., Beresini, M.H., de Leon Boenig, G., Bronner, S.M., Chen, K., Chen, Z., Choo, E.F., Crawford, T.D., Cyr, P., Kaufman, S., Li, Y., Liao, J., Liu, W., Ly, J., Murray, J., Shen, W., Wai, J., Wang, F., Zhu, C., Zhu, X., Magnuson, S., Design and Synthesis of A Biaryl Series As Inhibitors for the Bromodomains of CBP/P300, *Bioorganic & Medicinal Chemistry Letters* (2017), doi: <https://doi.org/10.1016/j.bmcl.2017.11.025>

This is a PDF file of an unedited manuscript that has been accepted for publication. As a service to our customers we are providing this early version of the manuscript. The manuscript will undergo copyediting, typesetting, and review of the resulting proof before it is published in its final form. Please note that during the production process errors may be discovered which could affect the content, and all legal disclaimers that apply to the journal pertain.



**Design and Synthesis of A Biaryl Series As Inhibitors for the Bromodomains of
CBP/P300**

Kwong Wah Lai,^{at} F. Anthony Romero,^{b†} Vickie Tsui,^{b*} Maureen H. Beresini,^b
Gladys de Leon Boenig,^b Sarah M. Bronner,^b Kevin Chen,^a Zhongguo Chen,^a Edna F.
Choo,^b Terry D. Crawford,^b Patrick Cyr,^b Susan Kaufman,^b Yingjie Li,^a Jiangpeng Liao,^a
Wenfeng Liu,^a Justin Ly,^b Jeremy Murray,^b Weichao Shen,^a John Wai,^a Fei Wang,^a
Caicai Zhu,^a Xiaoyu Zhu,^a Steven Magnuson^{b*}

^aWuXi AppTec Co., Ltd. 288 Fute Zhong Road, Waigaoqiao Free Trade Zone,
Shanghai 200131, People's Republic of China.

^bGenentech, Inc., 1 DNA Way, South San Francisco, California 94080, United
States.

Abstract

A novel, potent, and orally bioavailable inhibitor of the bromodomain of CBP, compound **35** (GNE-207), has been identified through SAR investigations focused on optimizing a bicyclic heteroarene to replace the aniline present in the published GNE-272 series. Compound **35** has excellent CBP potency (CBP IC_{50} = 1 nM, MYC EC_{50} = 18 nM), a selectivity index of >2500-fold against BRD4(1), and exhibits a good pharmacokinetic profile.

Keywords: Bromodomain, CBP inhibitor, volume of distribution, half-life

Cyclic AMP response element binding protein, binding protein (CREBBP, CBP) and the highly homologous paralog E1A-associated protein of 300 kDa (EP300, P300) are co-activators of many different transcription factors.¹⁻⁵ Both CBP and P300 possess several structured regions, which include the histone acetyltransferase (HAT) domain that acetylates both histone and non-histone proteins, and an epigenetic “reader” bromodomain (BRD) that binds acetylated lysine (KAc).⁶ CBP/P300 bind to chromatin via their BRD, and once associated with chromatin this complex will recruit additional transcriptional machinery to modulate gene expression.⁷ SiteMap analysis predicts the BRD of CBP to be a druggable target and garners increased interest from design and selectivity perspectives.⁸ In fact, CBP and P300 have been implicated as potential oncology targets.⁹⁻¹² The BRD of CBP/P300 (hereafter together referred to as “CBP”) regulates *MYC*,¹³ a transcription factor and oncogene widely expressed in human cancer, which suggests a potential therapeutic strategy for targeting multiple myeloma and other lymphoid malignancies. In addition, we have described the ability of CBP bromodomain inhibitors to impair T_{reg} differentiation and suppressive function, and this activity could constitute a novel small molecule approach for cancer immunotherapy.¹⁴ Given these combined activities, the CBP BRD has emerged as an especially interesting new therapeutic target. To help unravel the biology and therapeutic potential of CBP, several research groups have discovered various chemical probes that inhibit the BRD of CBP.¹⁵⁻²³

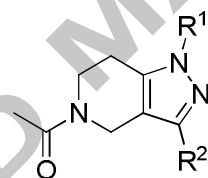
In a previous account, we reported the co-crystal structure of the screening hit **1** with the CBP BRD.¹⁶ The amide of **1** binds the KAc binding site, with the carbonyl making a canonical hydrogen bond interaction to Asn1168 and a water-mediated

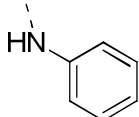
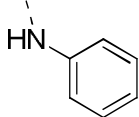
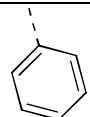
hydrogen bond to Tyr1125. The pyrazolopiperidine (PP) core is sandwiched between the gatekeeper (Val1174) and Leu1120, while the phenyl ring makes van der Waals interactions with the LPF shelf (Leu1109, Pro1110, Phe1111). Of particular interest was the aniline N-H that makes water-mediated interactions with the backbone of Pro1110 and the sidechain of Gln1113 (Figure 1A). Despite this structural role, the aniline carries a potential liability as a toxicophore via phase I oxidation that could lead to a highly electrophilic quinone imine metabolite. We recently reported on a highly potent and selective tetrahydroquinoline (THQ) series that was derived from **1**.²⁴ In parallel to the development of this THQ series, we embarked on an alternate strategy to replace the aniline with a bicyclic heteroarene. Here we describe the structure-based design of **35** (GNE-207), a potent and selective CBP inhibitor that exhibits a good pharmacokinetic (PK) profile.

We initially explored structure-activity relationships (SAR) on **2** containing a cyclopropylmethyl (*c*-Pr) moiety. The cyclopropylmethyl was derived from our earlier studies on the SAR of **1** in our progress towards the development of GNE-272.¹⁶ It was found that the cyclopropylmethyl substituent binds in the ZA loop region and improves CBP potency. To observe whether we could simply replace the aniline of **2**, we made compound **3**, which contained a phenyl substituent directly attached to the PP core. This compound retained CBP potency compared to **2** and maintained good ligand efficiency (LE). Encouraged by this result, we then attempted to increase the van der Waals interaction of **3** with Pro1110 by replacing the phenyl with an indole. Compound **4** had an 8-fold increase in CBP inhibitory potency. We hypothesized that the indole was important for stacking with Pro1110. To confirm this, we obtained a co-crystal structure

of **4** with the bromodomain of CBP (Figure 1B). As expected, the amide carbonyl makes a direct hydrogen bond to Asn1168 and water-mediated hydrogen bonds to Tyr1125. In addition, the indole A ring makes van der Waals interactions with C β and C γ of Pro1110 while the B ring *pi*-stacks with the amide plane formed by the carbonyl from Leu1109 and the nitrogen from Pro1110.²⁵ Meanwhile, the sidechain of Gln1113 rotated out to face solvent. Together these structural observations account for the potency gain observed and confirm the hypothesis that the water molecule ligating the aniline N-H on **1** and the receptor can be displaced.

Table 1. Initial Replacements of the Aniline



| Cmpd | R ¹ | R ² | CBP IC ₅₀ (μM) ^a | LE (CBP) |
|----------|----------------------|---|--|----------|
| 1 | H |  | 0.74 | 0.45 |
| 2 | CH ₂ c-Pr |  | 0.15 | 0.42 |
| 3 | CH ₂ c-Pr |  | 0.24 | 0.42 |

| | | | | |
|---|----------------------|--|-------|------|
| 4 | CH ₂ C-Pr | | 0.031 | 0.42 |
|---|----------------------|--|-------|------|

^aAll IC₅₀ values are reported as means of values from at least two determinations. TR-FRET assay with the isolated CBP bromodomain.

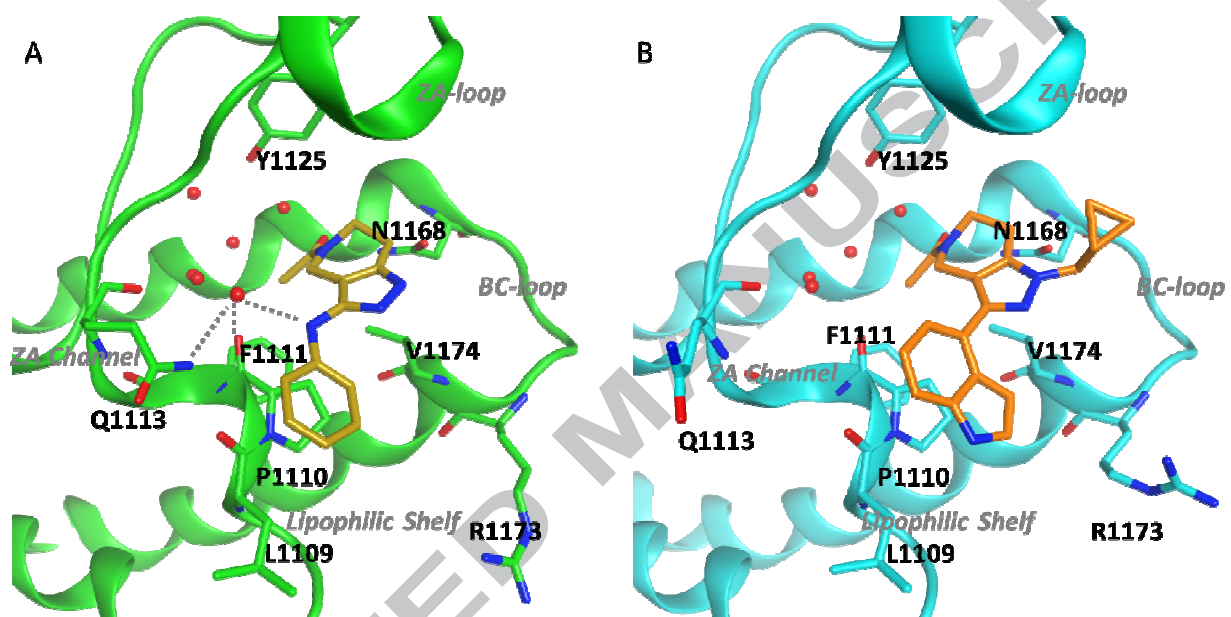
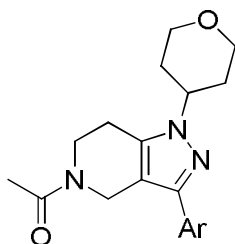
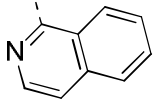


Figure 1. Co-crystal structures of (A) **1** in the CBP bromodomain with the ligand carbon atoms shown in yellow and the protein carbon atoms shown in green (2.3 Å resolution, PDB code 5KTU) and (B) **4** in the CBP bromodomain with the ligand carbon atoms shown in orange and the protein carbon atoms shown in cyan (1.4 Å resolution, PDB code 6ALC). Specific residues and structural features are displayed and labeled, and the water-mediated hydrogen bond network between **1** and Gln1113 is depicted as grey dashed lines.

Table 2. Heterocyclic Derivatives That Explore the LPF Shelf



| Cmpd | Ar | CBP IC ₅₀ (μM) ^a | BRD4 IC ₅₀ (μM) ^a | Selectivity ^b |
|------|----|--|---|--------------------------|
| 5 | | 0.12 | 4.7 | 39 |
| 6 | | 0.043 | 11 | 256 |
| 7 | | 0.079 | >20 | >253 |
| 8 | | 0.081 | >20 | >247 |
| 9 | | 0.03 | 14 | 467 |
| 10 | | 0.13 | 14 | 108 |
| 11 | | 0.09 | >20 | >222 |

| | | | | |
|-----------|---|------|-----|------|
| 12 |  | 0.19 | >20 | >105 |
|-----------|---|------|-----|------|

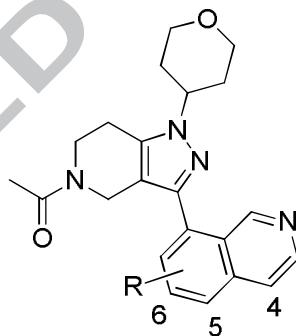
^aAll IC₅₀ values are reported as means of values from at least two determinations. TR-FRET assay with the isolated CBP or BRD4(1) bromodomain.

^bSelectivity is defined by [BRD4(1) IC₅₀ (μM) / CBP IC₅₀ (μM)].

We sought to improve the affinity of **4** and evaluate additional bicycles (Table 2). During our parallel work on the THQ series²⁴ we had discovered that a tetrahydropyran (THP) capped pyrazole appeared beneficial for potency, and thus we continued exploring bicycles with the THP in place. Additionally, at this stage, we started monitoring selectivity against bromodomain 1 of the bromodomain-containing protein 4 (BRD4(1)). Inhibition of the bromodomain and extra terminal (BET) family bromodomains has an overlapping phenotype with CBP and we were particularly focused on BRD4(1) (our surrogate for BET bromodomains) as the off-target. The indole **5** displayed an approximately 4-fold decrease in potency compared to **4**, but the reverse indole **6** gained back the CBP potency and showed improved BRD4(1) selectivity compared to **5**. We hypothesize that this SAR may result from a slight shift of the PP core due to the THP, which may affect the shape complementarity of the indole with CBP and BRD4(1). Compounds **7** and **8** were synthesized to evaluate whether an interaction between the ring carbonyl and Arg1173 can be made. Unfortunately, **7** and **8** were 2-fold less potent biochemically compared with indole **6**, indicating that the carbonyl may be too bulky to directly interact with the guanidine group of Arg1173. Next,

we envisioned that the more lipophilic isoquinoline could be a suitable chemotype to replace the indole since the weakly basic nitrogen atom on isoquinoline might be able to electronically interact with Arg1173 without the extra bulk offered by **7** and **8**. Moreover, the isoquinoline ring system could offer a vector to explore substitutions at the C3 position as a means of gaining potency. We were pleased to observe that isoquinoline **9** indeed increased CBP potency (4-fold) and further improved selectivity against BRD4(1) to >400-fold. Intrigued by these results, we evaluated other nitrogen-containing bicycles (**10–12**) and none appeared to match the potency of **9**. We chose to further examine SAR on **9**.

Table 3. Effect of Substitution on the Isoquinoline Ring of 9



| Cmpd | R | CBP IC ₅₀ (μ M) ^a | BRD4 IC ₅₀ (μ M) ^a | Selectivity ^b |
|-----------|------|---|--|--------------------------|
| 9 | H | 0.03 | 14 | 467 |
| 13 | 4-Cl | 0.042 | 14 | 333 |
| 14 | 4-Et | 0.038 | 15 | 395 |

| | | | | |
|-----------|----------------------|-------|-----|------|
| 15 | 4-CH ₂ OH | 0.081 | >20 | >247 |
| 16 | 4-OMe | 0.023 | 13 | 565 |
| 17 | 4-CN | 0.18 | >20 | >111 |
| 18 | 5-Cl | 0.09 | >20 | >222 |
| 19 | 5-Me | 0.013 | 7.7 | 592 |
| 20 | 5-Et | 0.031 | 8.5 | 274 |
| 21 | 5-CH ₂ OH | 0.065 | >20 | >308 |
| 22 | 5-OMe | 0.027 | 11 | 407 |
| 23 | 5-CN | 0.28 | >20 | >71 |
| 24 | 6-Cl | 0.17 | 19 | 112 |
| 25 | 6-Me | 0.058 | 12 | 207 |
| 26 | 6-Et | 0.024 | 7.8 | 325 |
| 27 | 6-CH ₂ OH | 0.069 | >20 | >290 |
| 28 | 6-OMe | 0.069 | 8.9 | 129 |
| 29 | 6-CN | 0.65 | >20 | >31 |

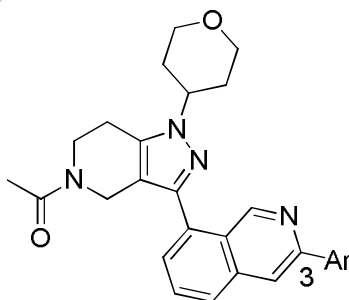
^aAll IC₅₀ values are reported as means of values from at least two determinations. TR-FRET assay with the isolated CBP or BRD4(1) bromodomain.

^bSelectivity is defined by [BRD4(1) IC₅₀ (μM) / CBP IC₅₀ (μM)].

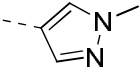
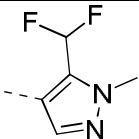
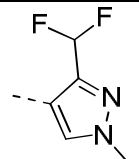
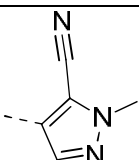
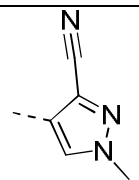
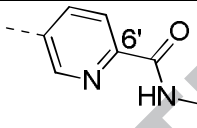
We systematically explored whether substitution off the isoquinoline ring of **9** could improve CBP potency and maintain selectivity against BRD4(1). Based upon models, it was anticipated that the addition of small substituents to the 4-, 5- and 6-

positions of the isoquinoline system could favorably enhance potency. Interestingly, a significant electronic effect was noted (Table 3). CBP potency remained largely unaffected when the 4-, 5- and 6-positions of the isoquinoline were substituted with weakly electron-withdrawing or electron-donating groups (F, Cl, Me, Et and OMe). However, when a strongly electron withdrawing cyano group was introduced, a significant reduction in potency was observed. There are multiple hypotheses for the drop in potency observed in cyano analogs (**17**, **23** and **29**) based on modeling studies. The cyano group could potentially weaken the aromatic-proline²⁵ interaction formed between the isoquinoline and Pro1110. Alternatively, the cyano group could be too polar for the Leu1109 sidechain in the case of 4- or 5-substitutions (**17** and **23**) or for the C β and Cy on Gln1113 in the case of the 6-sustitution (**29**).

Table 4. Heterocyclic Derivatives That Explore the LPF Shelf



| Cmpd | Ar | CBP IC ₅₀ (μ M) ^a | BRD4 IC ₅₀ (μ M) ^a | MYC EC ₅₀ (μ M) ^a | LM Cl _{hep} ^b M / R / H |
|------|----|---|---|---|--|
| | | | | | |

| | | | | | |
|----|---|--------|-----|-------|---------------|
| 30 |  | 0.0012 | 2.5 | 0.032 | 20 / 18 / 8.3 |
| 31 |  | 0.0028 | 3.3 | 0.11 | 51 / 22 / 16 |
| 32 |  | 0.0033 | 2.8 | 0.22 | 38 / 22 / 13 |
| 33 |  | 0.0033 | 6.7 | 0.076 | 36 / 20 / 11 |
| 34 |  | 0.0024 | 3.8 | 0.28 | 32 / 45 / 11 |
| 35 |  | 0.0012 | 3.2 | 0.018 | 36 / 15 / 9.3 |

^aAll IC₅₀ and EC₅₀ values are reported as means of values from at least two determinations. TR-FRET assay with the isolated CBP or BRD4(1) bromodomain. MYC expression in MV-4-11 cells. ^bMouse (M), rat (R), human (H) liver microsome-predicted hepatic clearance (mL/min/kg).

In order to increase interaction within the LPF shelf we introduced heterocycles to the 3-position of the isoquinoline linker (Table 4). Introduction of an *N*-methylpyrazole to **9** led to 30-fold enhancement in CBP potency compared to the parent **9**. At

this point we started monitoring liver microsome stability and **30** exhibited good metabolic stability in various species. Next, we incorporated a functional group (e.g., CHF₂ and CN) onto the distal pyrazole ring in an attempt to further interact with Arg1173. Unfortunately, there was a 2- to 3-fold decrease in CBP potency (**31–34**) compared to **30**. The binding mode of **30** was elucidated by crystallography (Figure 2). The PP core resides in KAc-binding pocket as expected, with the carbonyl interacting directly with Asn1168 and via a water molecule with Tyr1125. As predicted during the compound design process, the nitrogen atom of the isoquinoline ring engages in hydrogen bond interaction with Arg1173. Also, as in the structure with **4**, another compound without the aniline, the sidechain of Gln1113 is rotated and faces the solvent (Figure 2A). One face of the isoquinoline and *N*-methylpyrazole resides on the lipophilic shelf and makes van der Waals interactions with Leu1109 and Pro1110, while the other face is mostly solvent-exposed (Figure 2B).

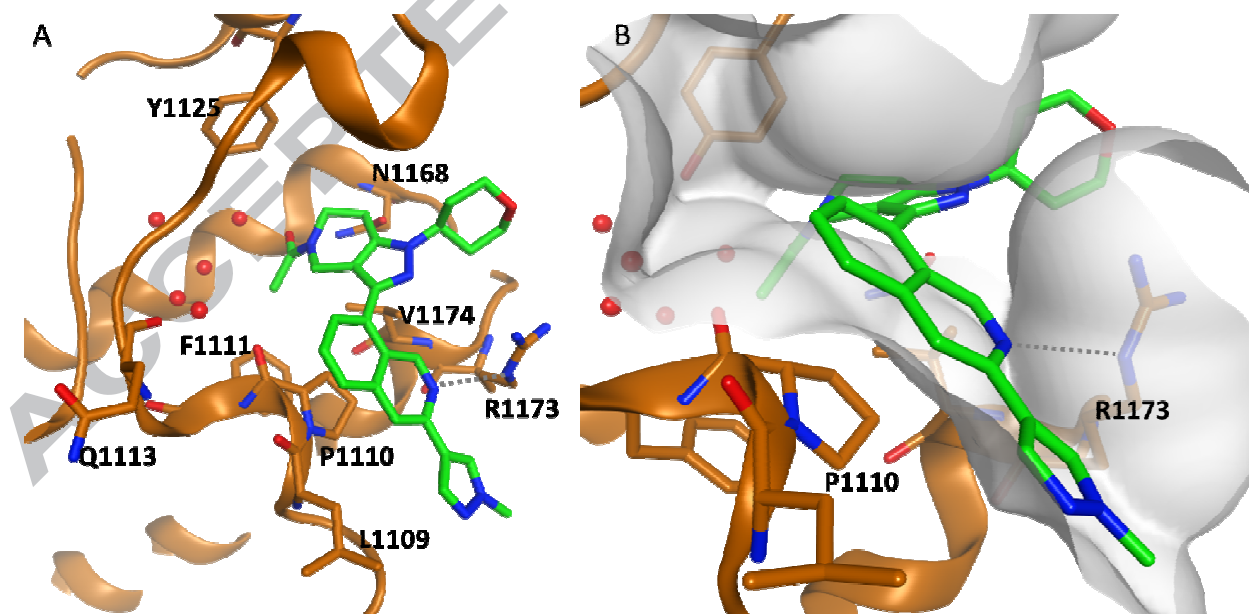


Figure 2. Co-crystal structure of **30** in the CBP bromodomain (1.6 Å resolution, PDB code: 6ALB) displaying the ligand in green and CBP ribbons in brown. The hydrogen bond between Arg1173 and nitrogen of isoquinoline is shown as grey dashed lines. (A) Residues discussed in the text are shown as sticks and labeled, and conserved water molecules are shown as red spheres. (B) The solvent-accessible surface area of the binding site is shown as in grey.

It was at this time during the work on the heterocyclic modification of **30** that we had identified GNE-781 (**36**), a highly potent and selective lead compound in the aforementioned THQ series (Table 5).²⁴ A concern for GNE-781 was the short half-life that it exhibited, which was in part due to the low volume of distribution. Introduction of basicity has been shown to increase half-life.²⁶ In order to test this hypothesis, we obtained mouse PK for **30** (containing a weakly basic amine), and we were pleased to observe that the volume of distribution increased as well as the half-life, albeit by a small amount, relative to **36**. To explore the possibility of increasing the half-life further, we anticipated that replacement of the distal pyrazole with an additional weakly basic *meta*-linked pyridine would improve the volume of distribution while retaining the desirable conformation of the molecule.^{25,26} Furthermore, introduction of an electron-withdrawing amide group could potentially increase the metabolic stability of the pyridine ring and, based on modeling, the 6'-position of the pyridine is solvent exposed and can accommodate the amide (Figure 3). Consistent with our modeling hypothesis, pyridine **35** had comparable CBP and *MYC* potencies relative to GNE-781, and exhibited ~2500-fold selectivity against BRD4. Though **35** has one additional hydrogen-bond donor compared with **30**, its permeability was maintained, which could be

associated with the intra-molecular hydrogen bond between amide N-H and the nitrogen atom of the distal pyridine. The methyl urea on GNE-781 was evaluated on compound **35** and similar potency and selectivity were observed for this compound. However, the compound had low permeability and minimal oral exposure and thus we chose to further evaluate compound **35**.

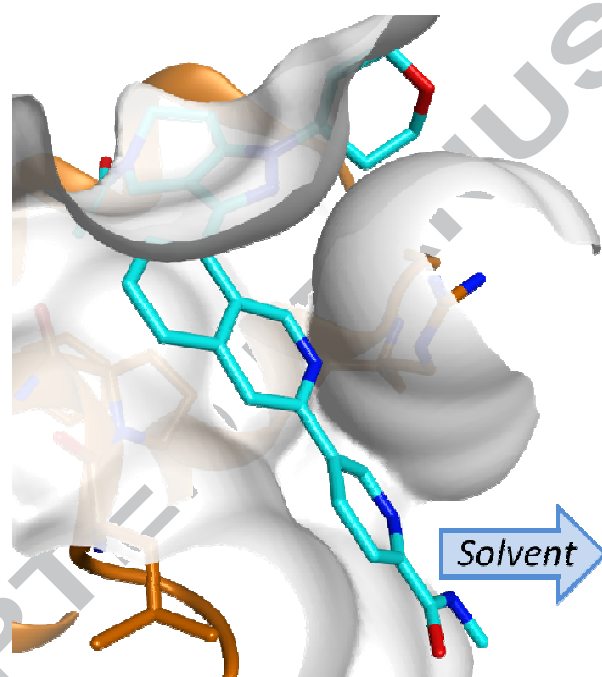


Figure 3. Compound **35** modeled into the CBP bromodomain (see Supplemental Information on methods).

Compound **35** exhibited moderate clearance in PK, with acceptable oral bioavailability. Evaluation using the BROMOscan technology platform (Figure 4) revealed the exquisite selectivity of **35**. Additionally, when tested (full details in

Supporting Information) in a Cerep off-target screening panel (10 μ M, 43 receptors), **35** did not inhibit any target at >40%. It was at this point in our discovery program that GNE-781 became the compound we focused our attention on due to its exquisite potency, selectivity and PK profile. While compound **35** did have an improved half-life compared to GNE-781, the selectivity for CBP over BRD4 was not as good as the selectivity that GNE-781 possessed. Not only did GNE-781 have exquisite potency and selectivity, it was also found to be non-CNS penetrant, an attribute that we wanted in our molecules. Further safety evaluation and brain penetration of **35** was never pursued, however, compound **35** became an instrumental in vitro tool representing a distinct chemical series.

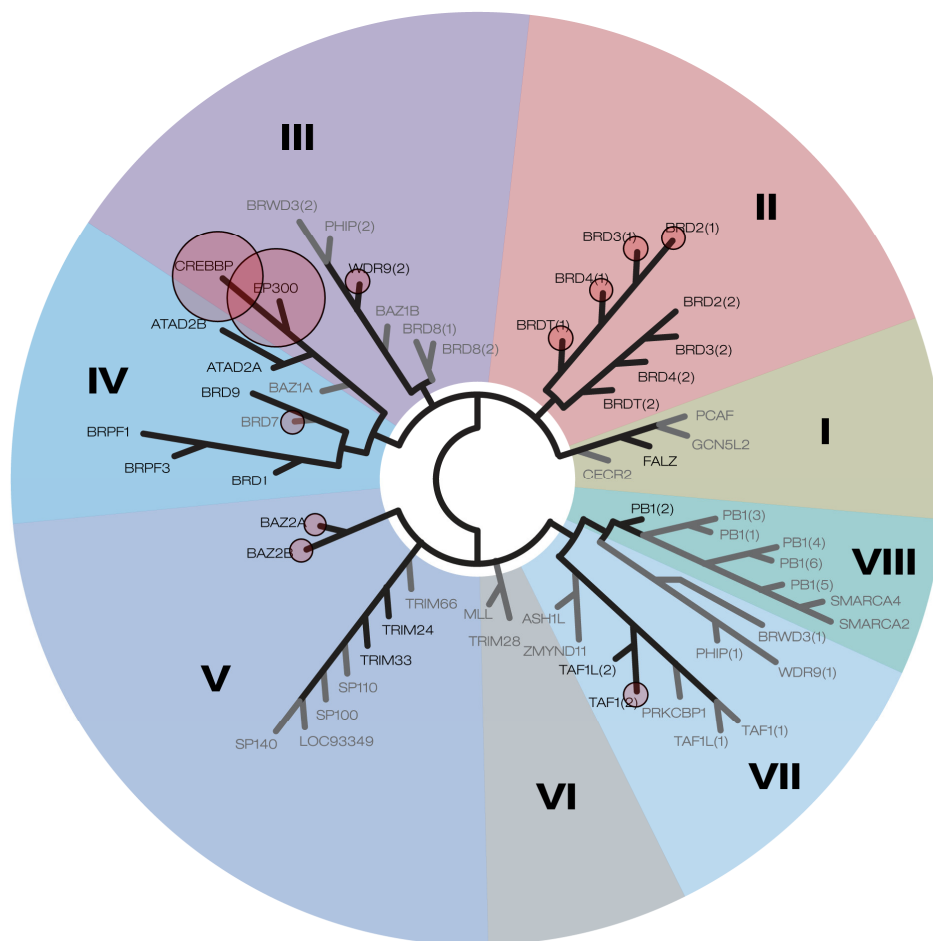
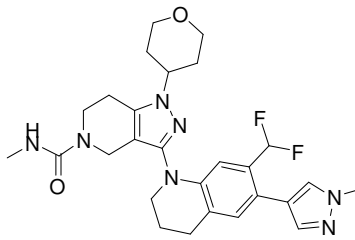
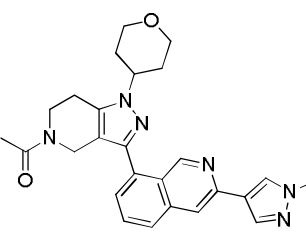
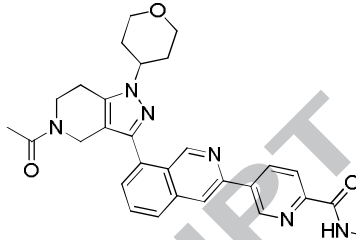


Figure 4. Broad Bromodomain Profile of **35**. K_d values obtained for **35** across a broad panel of bromodomains as assayed with the BROMOscan platform; the assay is based on competition between compound and affinity resin for binding to soluble DNA-tagged bromodomains. Bromodomains in black were included in the screen and those in grey were not. The two large red circles indicate K_d values of <1 nM and small red circles indicate K_d values of 1–3 μ M. If not marked by a circle then K_d values are > 3 μ M. For details see Supporting Information.

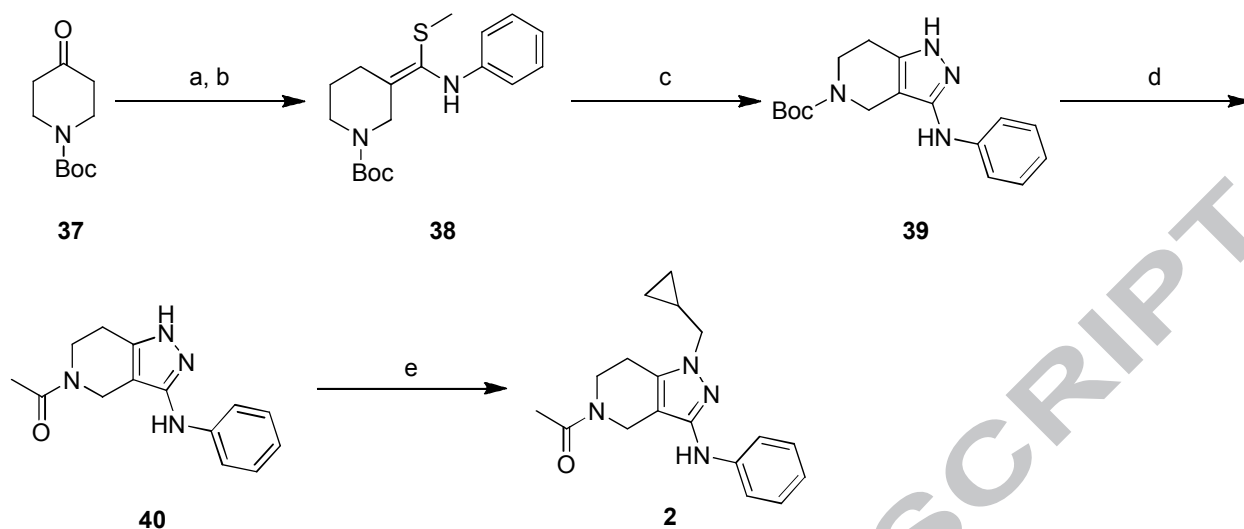
Table 5. Overall Profile of 30, 35 and 36

| Cmpd | 36 (GNE-781) | 30 | 35 (GNE-207) |
|--|---|--|---|
| Structure |  |  |  |
| CBP IC ₅₀ (nM) ^a | 0.9 | 1.0 | 1.0 |
| BRD4 IC ₅₀ (nM) ^a | 5,100 | 2,500 | 3,100 |
| Selectivity ^b | 5,670 | 2080 | 2580 |
| MYC EC ₅₀ (nM) ^a | 6.6 | 32 | 18 |
| MDCK P _{app} . A : B (x 10 ⁻⁶ cm/s) ^c | 19 | 10 | 12 |
| PPB (%) ^d M/R/H | 94 / 94 / 84 | 85 / 76 / 70 | 90 / 96 / 95 |
| LM Cl _{hep} (mL/min/kg) ^e M/R/H | 35 / 18 / 10 | 20 / 18 / 8 | 36 / 15 / 9 |
| Hep Cl _{hep} (mL/min/kg) | <21 / <10 / <6 | <21 / 14 / <6 | <21 / 10 / <6 |

| M/R/H | | | |
|-------------------------------------|-----|-----|-----|
| kSol (μM) ^g | 95 | 92 | 66 |
| CL (mL/min/kg) <i>h</i> | 5.2 | 11 | 18 |
| V _{ss} (L/kg) | 0.6 | 1.3 | 2.8 |
| T _{1/2} (h) | 1.4 | 1.6 | 2 |
| F (%) | 73 | 67 | 50 |

^aAll IC₅₀ and EC₅₀ values are reported as means of values from at least two determinations. TR-FRET assay with the isolated CBP or BRD4(1) bromodomain. MYC expression in MV-4-11 cells. ^bSelectivity is defined by [BRD4(1) IC₅₀ (μM) / CBP IC₅₀ (μM)]. ^cMDCK cell line; apical-to-basolateral; units = $\times 10^{-6}$ cm s⁻¹. ^dMouse (M), rat (R) and human (H) plasma protein binding. ^eMouse (M), rat (R) and human (H) liver microsome-predicted hepatic clearance. ^fMouse (M), rat (R) and human (H) hepatocyte-predicted hepatic clearance. ^gKinetic solubility was measured at pH 7.4 in PBS buffer. ^hMouse PK was performed in CD-1 mice; compounds were dosed iv (1 mg kg⁻¹) as PEG400/H₂O (35/65) solution and po (5 mg kg⁻¹) as an aqueous suspension with 0.2% Tween 80.

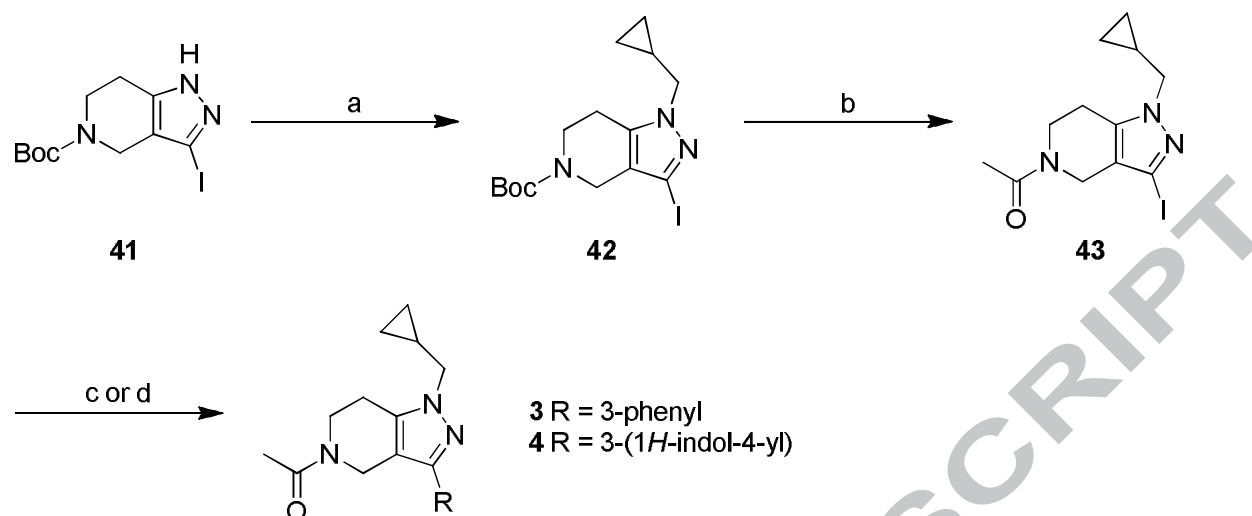
Scheme 1. Synthesis of 2



Reagents and conditions: (a) isothiocyanto-3-methylbenzene, KO^tBu, THF, rt; (b) CH₃I, 40 °C, 97%; (c) hydrazine monohydrate, EtOH, 85 °C, 97%; (d) i. HCl, EtOAc, rt, ii. Ac₂O, TEA, DCM, rt, 98%; (e) (bromomethyl)cyclopropane, Cs₂CO₃, DMF, 100 °C, 27%.

The synthesis of **2** is depicted in Scheme 1. Treatment of piperidone **37** with 1-isothiocyanto-3-methylbenzene followed by alkylation with methyl iodide produced **38**. Cyclization of **38** with hydrazine afforded Boc protected pyrazolopiperidine **39**. Deprotection of the Boc group followed by acetylation yielded acetamide **40**. Final *N*-alkylation of **40** with (bromomethyl)cyclopropane produced **2**.

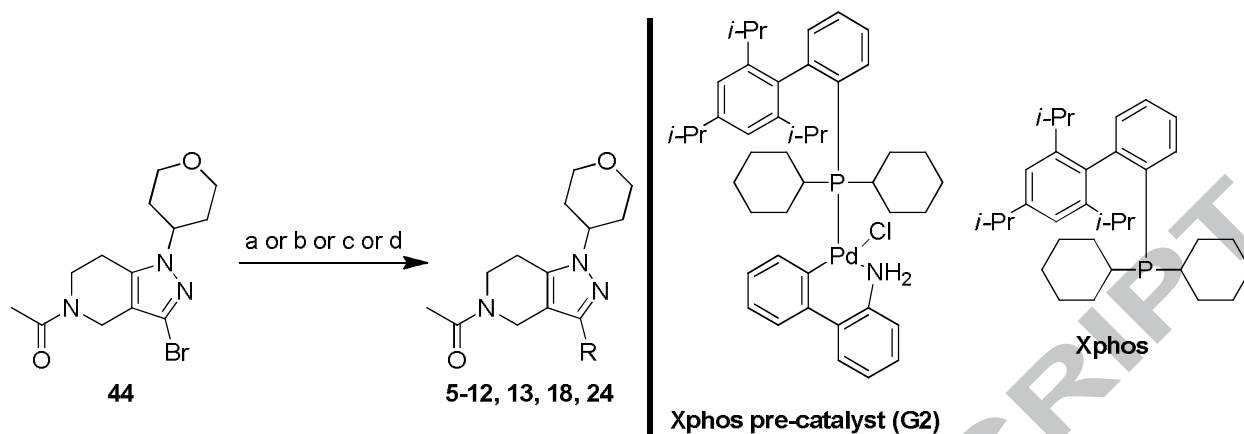
Scheme 2. Synthesis of **3** and **4**



Reagents and conditions: (a) (bromomethyl)cyclopropane, K_2CO_3 , DMF, 80 °C; (b) i. HCl, EtOAc, rt, ii. Ac_2O , TEA, DMF, rt, 99%; (c) phenylboronic acid, $\text{Pd}(\text{dppf})\text{Cl}_2$, Na_2CO_3 , dioxane, H_2O , 100 °C, 10%; (d) 4-(4,4,5,5-tetramethyl-1,3,2-dioxaborolan-2-yl)-1*H*-indole, $\text{Pd}(\text{PPh}_3)_4$, Cs_2CO_3 , dioxane, H_2O , 100 °C, 16%.

Compounds **3** and **4** were prepared according to Scheme 2. The synthesis of **41** has been described in the literature.²⁷ *N*-alkylation of **41** with (bromomethyl)cyclopropane produced **42**. Boc deprotection and *N*-acetylation gave acetamide **43**. A palladium-catalyzed Suzuki strategy was utilized to couple the iodo-PP core with the boronic acid or boronate ester to produce **3** and **4**.

Scheme 3. Synthesis of Compounds 5–12, 13, 18 and 24



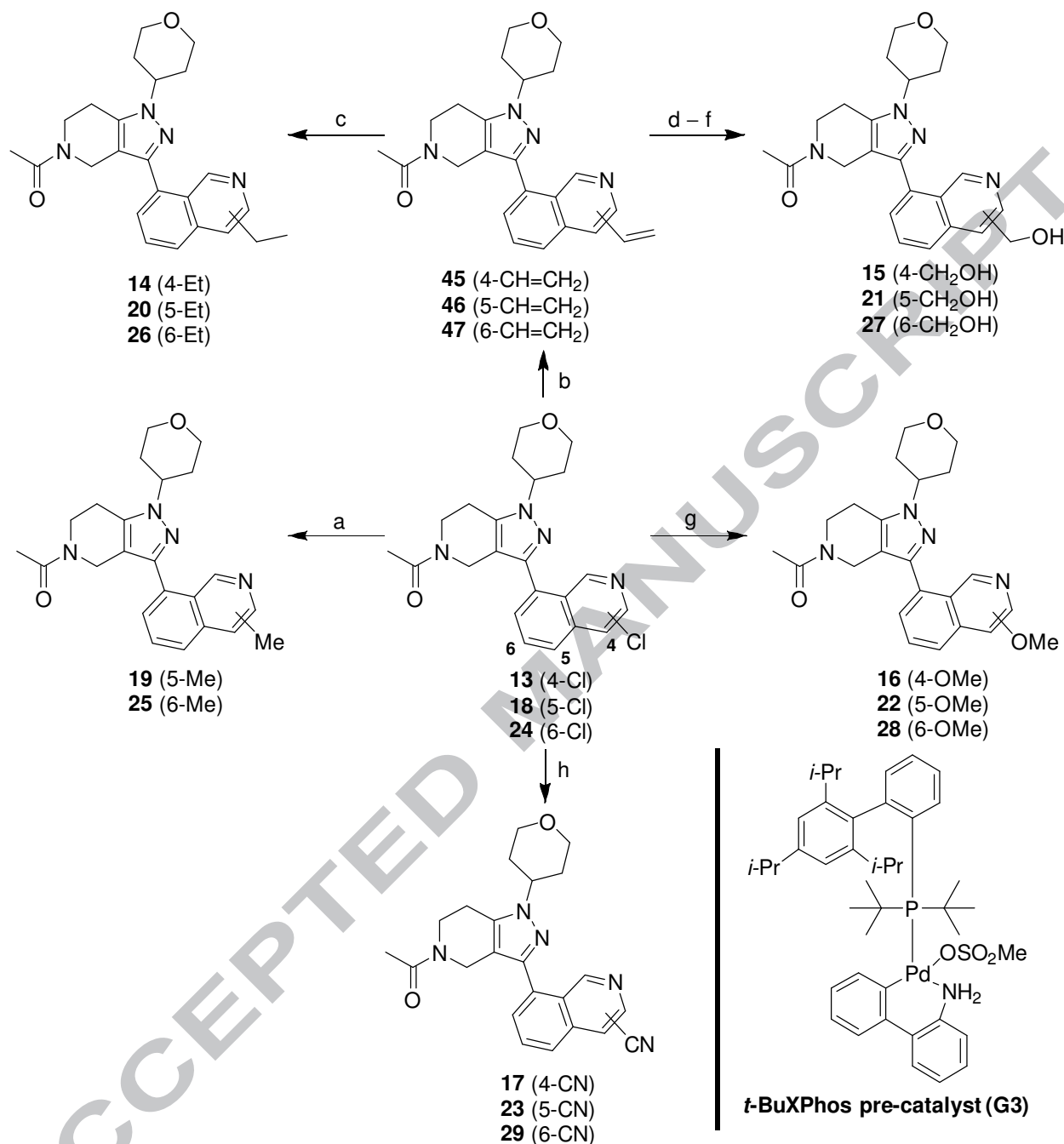
- 5** R = 3-(1*H*-indol-4-yl) (69%)^a
6 R = 3-(1*H*-indol-3-yl) (35%)^b
7 R = 3-(isoquinolin-3(2*H*)-one-5-yl) (2%)^c
8 R = 3-(1,2-dihydroisoquinolin-3(4*H*)-one-5-yl) (20%)^c
9 R = 3-(isoquinolin-8-yl) (53%)^c
10 R = 3-(quinolin-4-yl) (50%)^a
11 R = 3-(isoquinolin-4-yl) (90%)^a
12 R = 3-(isoquinolin-1-yl) (45%)^c
13 R = 3-(4-chloroisoquinolin-8-yl) (35%)^d
18 R = 3-(5-chloroisoquinolin-8-yl) (46%)^d
24 R = 3-(6-chloroisoquinolin-8-yl) (33%)^d

Reagents and conditions: (a) i. Ar–B(OH)₂, XPhos pre-catalyst (G2) (5 mol %), XPhos (5 mol %), K₃PO₄ (2.5 equiv), dioxane/H₂O, 60 °C; (b) i. (1-(*tert*-butoxycarbonyl)-1*H*-indol-3-yl)boronic acid, XPhos pre-catalyst (G2) (4 mol %), Na₂CO₃ (2.5 equiv), THF/H₂O, 60 °C, ii. TFA, DCM, rt; (c) i. B₂Pin₂, XPhos pre-catalyst (G2) (3 mol %), XPhos (6 mol %), KOAc (3 equiv), dioxane, 80 °C, ii. Ar–Br, XPhos pre-catalyst (G2) (4 mol %), K₃PO₄ (2.5 equiv), dioxane/H₂O, 90 °C (d) i. B₂Pin₂, Pd(dppf)Cl₂ (10 mol %), KOAc (3 equiv), dioxane, 80 °C, ii. Ar–Br, Pd(dppf)Cl₂ (10 mol %), K₃PO₄ (3 equiv), dioxane/H₂O, 80 °C.

The general synthetic route used for the preparation of compounds listed in Table 1 and chloro-isoquinolines **13**, **18** and **24** is depicted in Scheme 3. Synthesis of **44** has been described in the literature.²⁴ Bromide **44** was treated with a heteroarene boronic acid

and XPhos pre-catalyst (G2) to give **5**, **6**, **10** and **11**. Alternatively, the bromo-PP core **44** was first treated with bis(pinacolato)diboran and XPhos pre-catalyst to give the corresponding boronate ester (structure not shown), which was immediately cross-coupled with the heteroaryl bromides under Suzuki conditions to give **7–9**, **12**, **13**, **18** and **24**.²⁸

Scheme 4. Synthesis of Compounds 14–17, 19–23 and 25–29

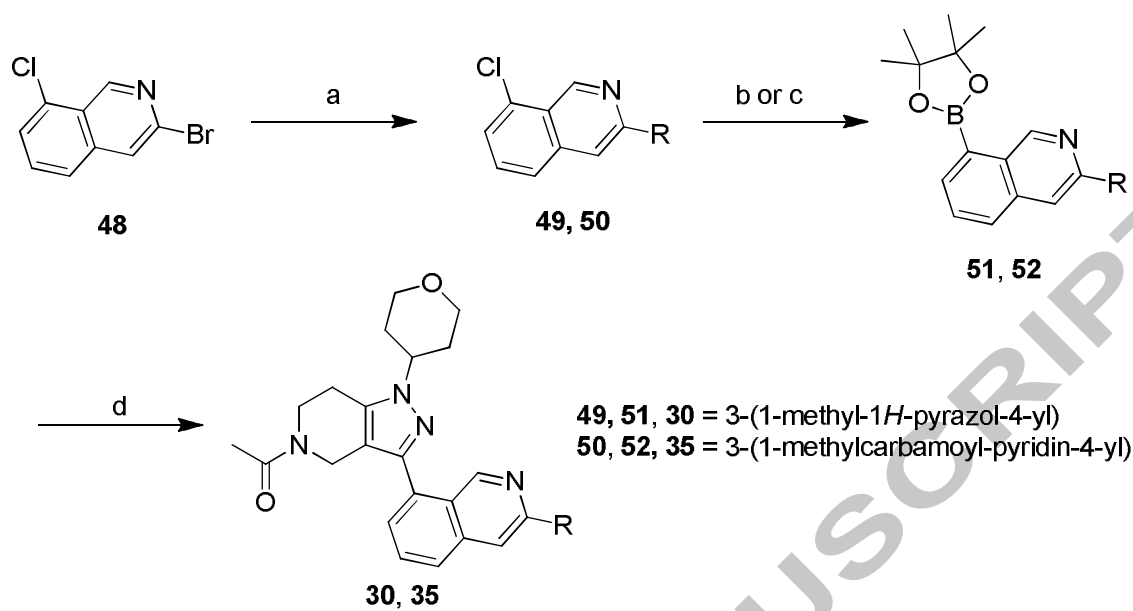


Reagents and conditions: (a) MeBF₃K (1 equiv), Pd(OAc)₂ (1 equiv), butyl-di-1-adamantylphosphine (1 equiv), Cs₂CO₃ (1 equiv), PhMe/H₂O, 80 °C, 8–9%. (b) 4,4,5,5-tetramethyl-2-vinyl-1,3,2-dioxaborolane, XPhos pre-catalyst (G2) (10 mol %), XPhos (10 mol %), Na₂CO₃ (2 equiv), THF/H₂O, 60 °C, 51–91%; (c) 10% Pd/C (5 mol %), H₂ (15 psi), MeOH, rt, 3–13%. (d) OsO₄, THF/H₂O, rt; (e) NaIO₄, THF/H₂O, rt; (f) NaBH₄,

MeOH, 0 °C, 3–7% three steps. (g) MeOH (5 equiv), *t*-BuXPhos pre-catalyst (G3) (20 mol %), *t*-BuXPhos (20 mol %), *t*-BuONa (1.4 equiv), dioxane, 50 °C, 7–9%. (h) K₄Fe(CN)₆·3H₂O (0.5 equiv), *t*-BuXPhos pre-catalyst (G3) (10 mol %), *t*-BuXPhos (10 mol %), KOAc (3 equiv), dioxane/H₂O, 120 °C, 7–10%.

As outlined in Scheme 4, chloro-substituted isoquinoline (**13**, **18** and **24**) served as the key intermediate toward the syntheses of methyl, ethyl, hydroxyl, methoxy and cyano variants. Briefly, Suzuki cross-coupling of **13** and **18** with the methyl Molander salt led to **19** and **25**. Cross-coupling of **13**, **18** and **24** with vinyl boronate afforded **45**, **46** and **47**, which upon hydrogenation produced the ethyl analogs **14**, **20** and **26**, respectively. The vinyl intermediates were transformed to the hydroxymethyls (**15**, **21** and **27**) by a sequence of dihydroxylation, oxidative cleavage and reduction. To convert chloride (**13**, **18** and **24**) to the corresponding methoxyl analogs (**16**, **22** and **28**), a MeOH and *t*-BuXPhos pre-catalyst combination was used.²⁹ Palladium-catalyzed cyanation of **13**, **18** and **24** led to **17**, **23** and **29**, respectively.³⁰

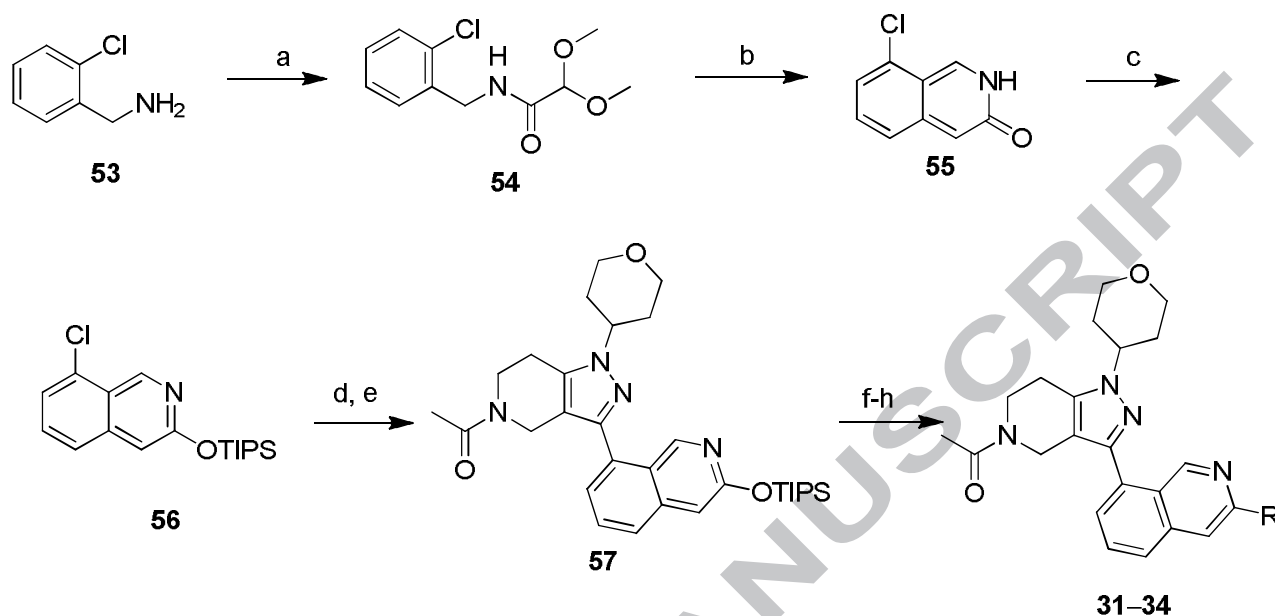
Scheme 5. Synthesis of Compounds 30 and 35



Reagents and conditions: (a) Ar-Bpin, Pd(dppf)Cl₂ (5 mol %), Na₂CO₃ (3 equiv), dioxane/H₂O, 90 °C, 81–92%; (b) **49**, B₂Pin₂, Pd(dppf)Cl₂ (5 mol %), KOAc (3 equiv), DMF, 90 °C, 24%; (c) **50**, B₂Pin₂, XPhos pre-catalyst (G2) (10 mol %), XPhos (10 mol %), KOAc (3 equiv), dioxane, 90 °C, 84%; (d) **44**, Xphos pre-catalyst (G2) (10 mol %), XPhos (10 mol %), Na₂CO₃ (3 equiv), THF/H₂O, 60 °C, 10–21%.

Scheme 5 shows the synthesis of analogs **30** and **35**. Commercially available 3-bromo-8-chloroisoquinoline **48** was subjected to chemo-selective Suzuki coupling with heteroaryl boronate esters to furnish **49** and **50**. The resultant chlorides (**49** and **50**) were converted to the corresponding boronate esters (**51** and **52**) that were subsequently subjected to Suzuki coupling with PP-bromide **44** to afford **30** and **35**, respectively.

Scheme 6. Synthesis of Compounds 31–34



Reagents and conditions: (a) methyl 2,2-dimethoxyacetate, TEA, MeOH, 80 °C, 84%;
 (b) H₂SO₄, H₂O, 0 °C–rt, 75%; (c) TIPS–Cl, 1*H*-imidazole, DMF, 0 °C–rt, 58%; (d)
 B₂Pin₂, XPhos pre-catalyst (G2) (10 mol %), XPhos (10 mol %), KOAc (3 equiv),
 dioxane, 80 °C; (e) **44**, XPhos pre-catalyst (G2) (10 mol %), K₃PO₄ (3 equiv),
 dioxane/H₂O, 90 °C, 28% from **56**; (f) TBAF, THF, rt, 75%; (g) TEA, PhN(SO₂CF₃)₂,
 DCM, rt, 29% from **57**; (h) Ar–Bpin, Xphos pre-catalyst (G2) (10 mol %), XPhos (10 mol
 %), Na₂CO₃ (3 equiv), THF/H₂O, 60 °C, 5–28%.

To expedite the distal heteroaryl SAR exploration, we also developed a route that enabled late stage installation of a functional group to the 3-position of the isoquinoline (Scheme 6). Benzyl amine **53** was treated with methyl 2,2-dimethoxyacetate and triethylamine in methanol to produce amide **54**, which upon treatment with H₂SO₄ furnished isoquinolin-3(2*H*)-one **55**. Treatment of **55** with TIPS-Cl and imidazole afforded **56** which was transformed to the corresponding boronate ester and then coupled with **44** under the similar Suzuki conditions to afford **57**. Desilylation of **57** with TBAF followed by triflation then subsequent Suzuki coupling with various heteroaryl boronate esters to give desired analogs **31–34**.

In summary, through structure-based design and optimization, a new class of isoquinoline-type CBP inhibitors has been discovered. We systematically examined the SAR on the C4, C5 and C6 positions of the isoquinoline. The introduction of the distal heterocycle to the C3 position of isoquinoline proved to be essential to achieve single-digit nM potency for CBP. The X-ray structure of compound **30** in complex with the CBP BRD was obtained and illustrated the interaction of the nitrogen of the isoquinoline ring with Arg1173. More strikingly, mouse PK results of selected inhibitors revealed that combination of isoquinoline and pyridine, as exemplified by compound **35**, can complement each other in increasing volume of distribution and half-life.

Author Information

Corresponding author

*V.T. E-mail: vickie.tsui@aya.yale.edu

*S.M. E-mail: magnuson.steven@gene.com

†These authors contributed equally.

Note

The author confirms that this article content has no conflicts of interest.

Acknowledgements

We thank Mengling Wong, Michael Hayes, and Amber Guillen for compound purification. Baiwei Lin, Deven Wang, and Yutao Jiang are acknowledged for analytical support. Grady Howes, Jan Seerveld, Hao Zheng, Ted Peters, and Gigi Yuen for help with compound management and logistics are also recognized.

References

- (1) Bannister AJ, Kouzarides T. The CBP Co-Activator Is a Histone acetyltransferase. *Nature* 1996;384:641–643.
- (2) Ogryzko VV, Schiltz RL, Russanova V, Howard BH, Nakatani Y. The transcriptional coactivators p300 and CBP are histone acetyltransferases. *Cell* 1996;87:953–959.
- (3) Vo N, Goodman RH. CREB-binding protein and p300 in transcriptional regulation. *J. Biol. Chem.* 2001;276:13505–13508.

- (4) Delvecchio M, Gaucher J, Aguilar-Gurrieri C, Ortega E, Panne D. Structure of the P300 Catalytic Core and Implications for Chromatin Targeting and HAT Regulation. *Nat. Struct. Mol. Biol.* 2013;20:1040–1046.
- (5) Mujtaba S, He Y, Zeng L, Yan S, Plotnikova O, Sachchidanand, Sanchez R, Zeleznik-Le NJ, Ronai Z, Zhou MM. Structural Mechanism of the Bromodomain of the Coactivator CBP in P53 Transcriptional Activation. *Mol. Cell* 2004;13:251–263.
- (6) Ito A, Lai CH, Zhao X, Saito S, Hamilton MH, Appella E, Yao T. P. p300/CBP-Mediated p53 Acetylation is commonly Induced by p53-activating Agents and Inhibited by MDM2. *EMBO J.* 2001;20:1331–1340.
- (7) Radhakrishnan I, Perez-Alvarado GC, Parker D, Dyson HJ, Montminy MR, Wright PE. Solution Structure of the KIX Domain of CBP Bound to the Transactivation Domain of CREB: A Model for Activator:Coactivator Interactions. *Cell* 1997;91:741–752.
- (8) Vidler LR, Brown N, Knapp S, Hoelder S. Druggability analysis and structural classification of bromodomain acetyl-lysine binding sites. *J. Med. Chem.* 2012;55:7346–7359.
- (9) Vervoorts J, Lüscher-Firzlaff JM, Rottmann S, Lilschkis R, Walsemann G, Dohmann K, Austen M, Lüscher B. Stimulation of c-MYC Transcriptional Activity and Acetylation by Recruitment of the Cofactor CBP. *EMBO Rep.* 2003;4:484–490.

- (10) Tomita A, Towatari M, Tsuzuki S, Hayakaw F, Kosugi H, Tamai K, Miyazaki T, Kinoshita T, Saito H. C-Myb Acetylation at the Carboxy-Termainl Conserved Domain by Transcriptional Co-Activator P300. *Oncogene* 2000;19:444–451.
- (11) Kim JH, Cho EJ, Kim ST, Youn HD. CtBP Represses p300-Mediated Transcriptional Activation by Direct Association with its Bromodomain. *Nat. Struct. Mol. Biol.* 2005;12:423–428.
- (12) Jin L, Garcia J, Chan E, la Cruz deC, Segal E, Merchant M, Kharbanda S, Haverty PM, Modrusan Z, Ly J, Choo EF, Kaufman S, Beresini MH, Romero FA, Magnuson S, Gascoigne KE. Therapeutic targeting of the CBP/p300 bromodomain blocks the growth of castration-resistant prostate cancer. *Cancer Res.* 2017; accepted.
- (13) Conery AR, Centore RC, Neiss A, Keller PJ, Joshi S, Spillane KL, Sandy P, Hatton C, Pardo E, Zawadzke L, Bommi-Reddy A, Gascoigne KE, Bryant BM, Mertz JA, Sims RJ. Bromodomain Inhibition of the Transcriptional Coactivators CBP/EP300 as a Therapeutic Strategy to Target the IRF4 Network in Multiple Myeloma. *eLife* 2016;5:e10483.
- (14) Ghosh S, Taylor A, Chin M, Huang H-R, Conery AR, Mertz JA, Salmeron A, Dakle PJ, Mele D, Côté A, Jayaram H, Setser JW, Poy F, Hatzivassiliou G, DeAlmeida-Nagata D, Sandy P, Hatton C, Romero FA, Chiang E, Reimer T, Crawford T, Pardo E, Watson VG, Tsui V, Cochran AG, Zawadzke L, Harmange JC, Audia JE, Bryant BM, Cummings RT, Magnuson SR, Grogan JL, Bellon SF, Albrecht BK, Sims RJ, Lora JM. Regulatory T Cell Modulation by CBP/EP300 Bromodomain Inhibition. *J. Biol. Chem.* 2016;291:13014–13027.

- (15) Taylor A M, Côté A, Hewitt MC, Pastor R, Leblanc Y, Nasveschuk CG, Romero FA, Crawford TD, Cantone N, Jayaram H, Setser J, Murray J, Beresini MH, de Leon Boenig G, Chen Z, Conery AR, Cummings RT, Dakin LA, Flynn EM, Huang OW, Kaufman S, Keller PJ, Kiefer JR, Lai T, Li Y, Liao J, Liu W, Lu H, Pardo E, Tsui V, Wang J, Wang Y, Xu Z, Yan F, Yu D, Zawadzke L, Zhu X, Zhu X, Sims RJ, Cochran AG, Bellon S, Audia JE, Magnuson S, Albrecht BK. Fragment-Based Discovery of a Selective and Cell-Active Benzodiazepinone CBP/EP300 Bromodomain Inhibitor (CPI-637). *ACS Med. Chem. Lett.* 2016;7,531–536.
- (16) Crawford TD, Romero FA, Lai KW, Tsui V, Taylor AM, de Leon Boenig G, Noland CL, Murray J, Ly J, Choo EF, Hunsaker TL, Chan EW, Merchant M, Kharbanda S, Gascoigne KE, Kaufman S, Beresini MH, Liao J, Liu W, Chen KX, Chen Z, Conery AR, Côté A, Jayaram H, Jiang Y, Kiefer JR, Kleinheinz T, Li Y, Maher J, Pardo E, Poy F, Spillane KL, Wang F, Wang J, Wei X, Xu Z, Xu Z, Yen I, Zawadzke L, Zhu X, Bellon S, Cummings R, Cochran AG, Albrecht BK, Magnuson S. Discovery of a Potent and Selective *in Vivo* Probe (GNE-272) for the Bromodomains of CBP/EP300. *J. Med. Chem.* 2016;59:10549–10563.
- (17) Popp TA, Tallant C, Rogers C, Fedorov O, Brennan PE, Müller S, Knapp S, Bracher F. Development of Selective CBP/P300 Benzoxazepine Bromodomain Inhibitors. *J. Med. Chem.* 2016;59:8889–8912.
- (18) Filippakopoulos P, Fedorov O, Picaud S, Cortopassi WA, Martin S, Tumber A, Philpott M, Wang M, Thompson AL, Heightman TD, Pryde DC, Cook A, Paton RS, Knapp S, Brennan PE, Conway SJ. A Series of Potent CREBBP Bromodomain Ligands

Reveals an Induced-Fit Pocket Stabilized by a Cation- π Interaction. *Angew. Chem. Int. Ed.* 2014;53:6126–6130.

(19) Fedorov O, Martin S, Singleton DC, Tallant C, Wells C, Picaud S, Philpott M, Monteiro OP, Conway SJ, Tumber A, Yapp C, Filippakopoulos P, Bunnage ME, Knapp S, Schofield CJ, Brennan PE. Discovery and Optimization of Small-Molecule Ligands for the CBP/P300 Bromodomains. *J. Am. Chem. Soc.* 2014;136:9308–9319.

(20) Unzue A, Xu M, Dong J, Wiedmer L, Spiliotopoulos D, Caffisch A, Nevado C. Fragment-Based Design of Selective Nanomolar Ligands of the CREBBP Bromodomain. *J. Med. Chem.* 2016;59:1350–1356.

(21) Picaud S, Fedorov O, Thanasopoulou A, Leonards K, Jones K, Meier J, Olzscha H, Monteiro O, Martin S, Philpott M, Tumber A, Filippakopoulos P, Yapp C, Wells C, Che KH, Bannister A, Robson S, Kumar U, Parr N, Lee K, Lugo D, Jeffrey P, Taylor S, Vecellio ML, Bountra C, Brennan PE, O'Mahony A, Velichko S, Müller S, Hay D, Daniels DL, Urh M, La Thangue NB, Kouzarides T, Prinjha R, Schwaller J, Knapp S. Generation of a Selective Small Molecule Inhibitor of the CBP/P300 Bromodomain for Leukemia Therapy. *Cancer Res.* 2015;75:5106–5119.

(22) Hammitzsch A, Tallant C, Fedorov O, O'Mahony A, Brennan PE, Hay DA, Martinez FO, Al-Mossawi MH, de Wit J, Vecellio M, Wells C, Wordsworth P, Müller S, Knapp S, Bowness P. CBP30, a Selective CBP/P300 Bromodomain Inhibitor, Suppresses Human Th17 Responses. *Proc. Natl. Acad. Sci. USA* 2015;112:10768–10773.

- (23) Denny RA, Flick AC, Coe JW, Langille J, Basak A, Liu S, Stock IA, Sahasrabudhe P, Bonin PD, Hay DA, Brennan PE, Pletcher MT, Jones LH, Chekler ELP. Structure-Based Design of Highly Selective Inhibitors of the CREB Binding Protein Bromodomain. *J. Med. Chem.* 2017;60:5349–5363.
- (24) Romero FA, Murray J, Lai KW, Tsui V, Albrecht BK, An L, Beresini MH, Boenig G, Bronner SM, Chan EW, Chen K, Chen Z, Choo E, Clagg K, Clark K, Crawford TD, Cyr P, Nagata DDA, Gascoigne KE, Grogan J, Hatzivassiliou G, Huang, W, Hunsaker TL, Kaufman S, Li Y, Liao J, Liu W, Ly J, Maher J, Merchant M, Ran Y, Taylor AM, Wai J, Wang F, Wei X, Yu D, Zhu BY, Zhu X, Magnuson S. GNE-781, A Highly Advanced Potent and Selective Bromodomain Inhibitor of CBP/P300. *J. Med. Chem.* Manuscript submitted. Manuscript ID: jm-2017-00796y.
- (25) Zondlo NJ. Aromatic-Proline Interactions: Electronically Tunable CH/ π Interactions. *Acc. Chem. Res.* 2013;46:1039–1049.
- (26) Smith DA, Beaumont K, Maurer TS, Di L. Volume of Distribution in Drug Design. *J. Med. Chem.* 2015;58:5691–5698.
- (27) Villa M, Abrate F, Fancelli D, Varasi M, Vulpetti A. Bicyclo-pyrazoles Active As Kinase Inhibitors, Process For Their Preparation And Pharmaceutical Compositions Comprising Them. WO2004014374A1.
- (28) Bruno NC, Tudge MT, Buchwald SL. Design and Preparation of New Palladium Precatalysts for C-C and C-N Cross-Coupling Reactions. *Chem. Sci.*, 2013;4:916–920.

(29) Bruno NC, Buchwald SL. Synthesis and application of palladium precatalysts that accommodate extremely bulky di-tert-butylphosphino biaryl ligands. *Org. Lett.*

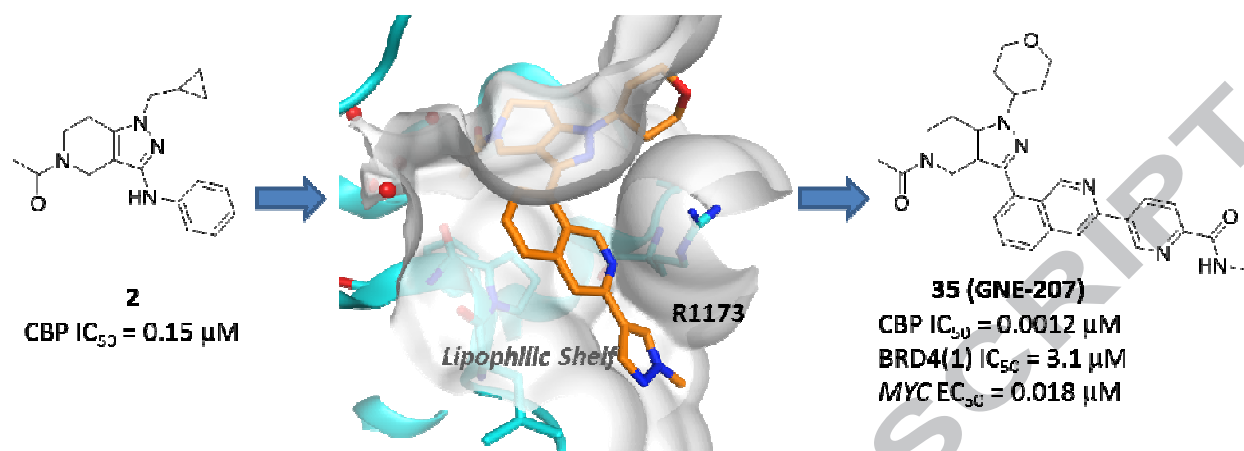
2013;15:2876–2879.

(30) Senecal TD, Shu W, Buchwald SL. A general, practical palladium-catalyzed cyanation of (hetero)aryl chlorides and bromides. *Angew. Chem. Int.*

Ed., 2013;52:10035–10039.

ACCEPTED MANUSCRIPT

Graphical Abstract



ACCEPTED MANUSCRIPT